Trop J Nat Prod Res, August 2024; 8(8):7947 - 7955 **ISSN 2616-0684 (Print)**
ISSN 2616-0692 (Electronic)

Tropical Journal of Natural Product Research

Available online at https://www.tjnpr.org

Original Research Article

Assessment of Antifungal Potentials of Ethanol Extract of *Cleistocalyx operculatus* Roxb Against *Cercospora nicotianae* for Pesticidal Applicability: *In Vitro* and *In Silico* Screening

Nguyen T. T. Hai[1], Thanh Q. Bui[1], Phan T. Quy[2], Nguyen V. Phu[3], Nguyen T. T. Thuy[4], Thi V. A. Nguyen[5], Nguyen T. Triet[6], Duy T. Pham[7], Van D. Tran[8], Nguyen T. A. Nhung[1]*

[1]*Department of Chemistry, University of Sciences, Hue University, Hue 530000, Vietnam*
[2]*Department of Natural Sciences & Technology, Tay Nguyen University, Buon Ma Thuot, Dak Lak 630000 Vietnam*
[3]*Faculty of Basic Sciences, University of Medicine and Pharmacy, Hue University, Hue 530000, Vietnam*
[4]*Faculty of Agronomy, University of Agriculture and Forestry, Hue University, Hue 530000, Vietnam*
[5]*Faculty of Engineering and Food Technology, University of Agriculture and Forestry, Hue University, Hue 530000, Vietnam*
[6]*Faculty of Traditional Medicine, University of Medicine and Pharmacy at Ho Chi Minh City, Ho Chi Minh City 700000, Vietnam*
[7]*Department of Health Sciences, College of Natural Sciences, Can Tho University, Can Tho 900000, Vietnam*
[8]*Department of Health Organization and Management, Can Tho University of Medicine and Pharmacy, Can Tho 900000, Vietnam*

ARTICLE INFO

Article history:
Received 29 March 2024
Revised 06 April 2024
Accepted 26 July 2024
Published online: 01 September 2024

ABSTRACT

Cleistocalyx operculatus is ubiquitous and known by folk experiences for its antimicrobial properties, thus promising as a low-cost green pesticide. In this work, the plant ethanol extract was investigated against *Cercospora nicotianae*, a pathogenic fungus implicated in the leaf spot in Pennywort. Characterisation of the plant extract showed 21 identifiable constituents (**1-21**), with the major components: 4',5'-dimethoxy-2'-hydroxy-4-methylchalcone (**21**; 41.71 %), phytol (**15**; 8.46 %), and 5.7-dimethoxyflavanone (**20**; 5.20 %). The *in vitro* antifungal screening of the extract revealed potent inhibitory capacity up to 7 days after inoculation (concentration = 9.54 mg.mL^{-1}). The inhibitory potential was predicted by docking simulation, i.e., 19-Q6DQW3 ($\overline{DS}$ -10.7 kcal.mol^{-1}; DS_{max} -12.7 kcal.mol^{-1}) > 21-Q6DQW3 ($\overline{DS}$ -10.3 kcal.mol^{-1}; DS_{max} -11.9 kcal.mol^{-1}) > 20-Q6DQW3 ($\overline{DS}$ -10.3 kcal.mol^{-1}; DS_{max} -11.7 kcal.mol^{-1}). The chemical potentiality was derived from quantum calculation, i.e., 22 (-1172.77 a.u.) > 21 ≈ 19 (approx. -1000 a.u.) > 20 (-ca. -950 a.u.) for chemical stability, and **3** (3.40 Debye), **15** (2.47 Debye), and **5** (2.03 Debye) for physical compatibility. The suitability for biological and pesticidal applications was justified by physicochemical analyses. The results revealed a firm correlation between the extracted major constituents (**20** and **21**) and the total antifungal activity against *C. nicotianae*, thus encouraging its local usage.

Keywords: *Cleistocalyx operculatus*, *Cercospora nicotianae*, *In vitro*, *In silico*, Antifungal activity

Introduction

Recently, organic agriculture has gained a notable surge in popularity worldwide, especially in horticulture. This requires safe and clean attributes to the consumers' health and environmental impacts, primarily regarding cultivar selection, soil fertilising, and pest controlling [1]. Pest control is often considered a process of high interest because it directly inoculates the pesticides into plants. Conventional practice pest control has long used synthetic chemicals in pest management as an inevitable routine, raising public concerns about their adverse effects. The contemporary approach utilises natural products known for high antimicrobial activities, killing and repelling pests, such as the essential oils of neem, lavender, garlic, chilli, wormwood, basil, etc.[2]

*Corresponding author. Email: ntanhung@hueuni.edu.vn
Tel: +84986980263

Citation: Hai NTT, Bui TQ, Quy PT, Phu NV, Thuy NTT, Nguyen TVA, Triet NT, Pham DT, Tran VD, Nhung NTA. Assessment of Antifungal Potentials of Ethanol Extract of *Cleistocalyx operculatus* Roxb Against *Cercospora nicotianae* for Pesticidal Applicability: *In Vitro* and *In Silico* Screening. Trop J Nat Prod Res. 2024; 8(8):7947-7955. https://doi.org/10.26538/tjnpr/v8i8.3

Official Journal of Natural Product Research Group, Faculty of Pharmacy, University of Benin, Benin City, Nigeria.

Shazia Parveen *et al.* (2014) reported broad screening research which revealed that five plant extracts: *Artemisia absinthium* L., *Rumex obtusifolius* L., *Taraxacum officinale* Weber ex Wiggers, *Plantago lanceolata* L., and *Malva sylvestris* L. exhibited significant inhibition against the mycelial growth of three fungi *Alternaria alternata* (Fr.) Keissler, *Penicillium expansum* Link ex Thom, and *Mucor piriformis* Fisher.[3] However, these sources are often not as bioavailable as required for the scale of industrial production, thus putting an almost prohibitive obstacle for practicable applications. *Cleistocalyx operculatus* (*Syzygium nervosum*) is known for its bioavailability and chemodiversity. The tree species are native to tropical regions of Asia and Australia, habiting widely from Guangdong and Guangxi (China) to the Northern Territory (Australia).[4] It is recognized as a medium-sized arborescent plant (ca. 10-m height) featured with pale brown bark and hue-green leaves. In particular, the leaves are elliptical, obovate, and glabrous (7-9 cm in length); the flowers are clustered and paniculate (4 petals); the fruits are concave-tip and wrinkle-texture ovolo, turning purplish upon ripening. The species contains various phytochemicals, e.g., oleanane-type triterpenes, sterols, flavanones, chalcon, triterpenic acid, *β*-sitosterol, ursolic acid, and essential oils.[5] However, this array of phytochemicals significantly challenges the attempts to specify the relationship between phytochemical characteristics and biological activities. The plant has also been evidenced for its antimicrobial properties. Evidence from folkloric usage revealed that *C. operculatus* leaves and buds are often brewed as an in-house herbal tea, known for stomachic benefits, while they also serve as effective remedies for

oxidative stress, skin inflammation, and wound infections. Pharmacological screening shows that the plant has been observed to exhibit antioxidant, antimicrobial, anti-mutagenic, anti-carcinogenic, anti-ageing, and neuroprotective properties.[6] Nevertheless, there is a lack of in-depth knowledge of the bioactivity of this plant in the literature. *C. operculatus* extracts were theoretically predicted to exhibit inhibitory activity against *Candida albicans*[7] and experimentally proven to enhance the fungicidal capacity of silver nanoparticles against *Colletotrichum camelliae.*[8] Therefore, the plant is of special interest as the source for bio-protectant applications because of its large morphology, ubiquitous distribution, and promising pesticidal activities. In horticultural cropping, leaf spots are one of the most common diseases with discoloured leaf lesions. The condition can lead to reduced plant vigour, leaf defoliation, and photosynthetic deficiency, thus resulting in yield loss if left untreated.[9] The causes are mainly related to the infection of fungi, bacteria, and viruses, especially fungi, which are often considered more challenging to treat than the latter. This is because eukaryotic cells generally have a more complex and rigid cellular structure compared to prokaryotic cells and viral capsids. Among the fungi commonly responsible for the diseases, the *Cercospora* species are known as the causative agents. These include 837 species (by July 2023) validated by the Global Biodiversity Information Facility (GBIF), with numerous undescribed species. In particular, *Cercospora nicotianae* is commonly recognised by *in situ* observations and widely subjected to *in vitro* settings.[10–13] Hence, this fungus is implicated as the potential representative of its genus in research studies.

Regarding mycology, *C. nicotianae* has recently been of special interest due to its genetic characterisation. Mainly, cercosporin, a perylenequinone, is responsible for light absorption and reaction with oxygen molecules to generate reactive oxygen species, and it is vital in the fungal virulence of infected plants.[14] Reactive oxygen species induce cell membrane peroxidation and cause damage to cellular components (i.e., lipids, proteins, and nucleic acids), leading to electrolyte leakage in host plants. This understanding led to significant efforts to investigate the cercosporin biosynthetic pathway and its regulation of *C. nicotianae.*[15,16] Results of a study revealed that the initial stage of cercosporin biosynthesis is catalysed by polyketide synthase CTB1 for the formation of nor-torlactone, a precursor for cercosporin production.[17,18] The findings suggest that this synthase is a promising target for inhibiting cercosporin activities, thus inhibiting the spreads and impacts of the fungi. The crystalline structure of *C. nicotianae* non-reducing polyketide synthase CTB1 has also been characterised and deposited onto the UniProtKB database under the entry Q6DQW3 (CTB1_CERNC). By leveraging computational power, *in silico* research offers notable advantages over traditional experimental methods, particularly in cost reduction and time efficiency. For instance, computer-aided drug design (CADD) facilitates the swift and reliable identification of potential drug candidates when various computational platforms are appropriately employed. Molecular docking simulations an integral part of CADD, represent a cost-effective technique for predicting binding mechanisms of ligand-protein inhibitory potentiality. Data derived from the physicochemical properties of potential inhibitors can complement the oversimplifications inherent in docking methods.[19,20] Besides, assessing the physical properties regarding solubility can provide a preliminary view of the biological persistence of the pesticidal candidates. Furthermore, quantum chemical computations can provide additional insights into properties such as chemo-physical suitability and intermolecular tendencies, thus conducive to evaluating ligand-protein inhibitory interaction. This combinatory and complementary model can result in well-rounded findings[21,22], hence offering a reliable assessment of biochemical compatibility. In this work, *C. operculatus* ethanol extract was subjected to an *in silico* investigation of its antifungal potential against *C. nicotianae*, mainly used in large-scale pesticide applications. Firstly, agricultural tests were deployed to confirm information on pathogenicity; experimental methods were used to prepare precursor materials, collect antifungal evidence, and determine compositional characteristics. Afterwards, different computer-based platforms were utilised to gather the chemical, biological, physiological, and pharmacological properties of the phytochemicals, with the resulting data being assessed for their potential inhibition and the pesticidal applicability of the total extract.

Materials and Methods

Plant collection and extraction

Cleistocalyx operculatus Roxb leaves were harvested from Thua Thien Hue province in June 2022. The samples were botanically identified by Dr. Nguyen Thanh Triet (Department of Traditional Pharmacy, University of Medicine and Pharmacy at Ho Chi Minh City) and deposited at the Department of Traditional Pharmacy, Faculty of Traditional Medicine (voucher no.: CLO-06-22). The collected leaves were washed, dried under the shade, ground to fine powders, and kept in a closed container until further use.

The powdered material (3 kg) was extracted by refluxing it with ethanol. A typical procedure for test samples proceeded on the raw-material powders (3 kg) with ethanol (150 mL; 70%) under the support of an ultrasonic bath (70 °C; 90 min); the remaining residues were filtered out and resent for the secondary extraction. Afterwards, the extracted products were combined and evaporated (60-70 °C); the final extract was stored for further studies while the condensed solvent was reclaimed for recycling processes.

Microorganisms

The pathogenic strain *C. nicotianae* was supplied by the Laboratory of Enzyme and Protein Technology at the Institute of Biotechnology, Hue University. The source of *C. nicotianae* was obtained by *in situ* extraction and lab-based culturing. First, Pennywort plants infected with the leaf-spot disease were collected from agricultural fields at Quang Tho Village, Quang Dien District, Thua Thien Hue Province (Vietnam). The fungal spore was isolated with PDA medium (Potato Dextrose Agar); in a typical procedure, a diseased plant tissue (approx. 10×10 mm) was disinfected using sodium hypochlorite (3% v/v; 2 min), rinsed using sterile distilled water (triplication), and dried using sterile paper napkins (room temperature; 20 min). The fungus was cultured in a laminar flow cabinet; in a typical procedure, the as-prepared tissues (5 samples) were transferred into a Petri dish containing PDA medium and incubated (28°C; 4-7 days) until the fungal growth was observable. The fungal isolates were purified using the hyphal tip technique; in a typical procedure, the colonies were transferred to a water-agar culture medium for growth (28°C; 3 days) before the hyphal tips were removed and transferred to PDA medium and left in refrigeration (5°C) for further use.

Microbial assay

In this assay, one-month-old Pennywort plants were inoculated with the pathogenic strain of *C. nicotianae* (four years old). The plants were transplanted into plastic pots (8 L) filled with a substrate mixture consisting of soil (80 %) and manure vermicompost-based material (20 %). Each pot was sprayed with a fungal solution (20 mL; 10^5 spores/mL) daily until the onset of leaf-spot symptoms; in addition, pure water was used in control samples. The treatments were carried out in five repetitions.

Antifungal activity assay

C. operculatus extract was used for the *in vitro* assay against *C. nicotianae* following the procedure proposed by Sánchez-Pérez *et al.*[23] Different concentrations of *C. operculatus* extract were mixed with PDA medium before transfer into sterile Petri plates and allowed solidify. Afterwards, the Petri plates were inoculated by placing a mycelial disc of *C. nicotianae* (5 mm) in the centre of each plate and incubated at 28°C. The control (PDA and the fungus) was set up without the addition of *C. operculatus* extract. All bioassays were in triplicates. The inhibitory effects of the extracts were evaluated by measuring colony diameter and recording the mycelial growth over a 7-day post-inoculation period. The results were expressed by percentage inhibition of mycelial growth compared to the negative control proposed by Pandey *et al*.[24]

Mycelial growth inhibition (%) = [(dc – dt)/dc] x 100 (%)

Where dc = control-based average diameter of fungal colony and dt = test-based average diameter of fungal colony.

Spectroscopic characterization
C. operculatus total extract was subjected to gas chromatography-mass spectrometry (GC-MS). Instrument: Agilent GC 7890B-MS 5975C; HP-5MS column (30 m × 0.25 mm × 0.25 µm); the carrier gas Helium (1.5 mL.min^{-1}). The GC temperature program: (i) commencing at 80°C (1 min); (ii) linearly increasing to 300°C (20°C.min^{-1}; 15 min); heat inlet at 250°C. The MS scanning configuration: line temperature at 280°C; ion-source temperature at 230°C; electron ionisation (EI) mode at 70 eV; batch scanning ranged 29-650 amu. The sample (1 µL) was split in a ratio of 20:1 before injection. The NIST-17 database was used as a reference for the phytoconstituents identified. All reagents, solvents, and chemicals were of analytical grade (Sigma-Aldrich, USA).

Computational input preparation
The data from the existing literature and experimental findings were used as the input for the computational screening. In particular, the chemical formulae of potential compounds (**1-21**) were obtained from GC-MS analysis and drawn using MOE 2022.10, while the protein assembly of *C. nicotianea* representative was referenced from a public protein bank, i.e., Non-reducing polyketide synthase CTB1 (UniProtKB: Q6DQW3 (CTB1_CERNC).

Docking simulation
A typical procedure of molecular docking simulation (MOE 2022.10[25]) follows three steps, i.e.: (i) Input preparation (configuration: protein active range 4.5 Å, ligand charge-assigning using Gasteiger-Huckel method); (ii) Docking simulation (configuration: retaining poses 10; solutions per iteration 1000; solutions per fragmentation 200); (iii) Re-docking iteration (threshold: root-mean-square deviation (RMSD) values < 2 Å; recommended by MOE).

Quantum calculation
The molecular chemical properties of the investigated structures were given by density functional theory (DFT) calculation using Gaussian 09 without symmetry constraints.[26] Level of theory M052X/6–311++G(d,p) and basis set def2-TZVPP[27] were selected. The converged geometries were checked for the structural global minimum on the potential energy surface (PES) by vibrational frequencies. The frozen-core approximation for non-valence-shell electrons was applied. The resolution-of-identity (RI) approximation was set. The frontier orbital analysis was carried out by NBO 5.1 at the level of theory M052X/def2-TZVPP.[28]

Physicochemical analysis
Drug-likeness properties of the phytochemicals were predicted by a combinational model. The parameters were the physical properties retrieved from QSARIS[29] (based on Gasteiger–Marsili method [30]). The references were from Lipinski's rule of five [31], which provides the theoretical criteria for a well membrane-permeable candidate, i.e., molecular mass < 500 Da; hydrogen-bond donors ≤ 5; hydrogen-bond acceptors ≤ 10; logP < +5.[32,33]

Results and Discussion

The pathogenic analysis followed Koch's postulates for pathogenicity identification.[34] The leaf-spot disease infection was assessed by the presence of limited and discoloured lesions on the selected Pennywort leaves. The infected parts were separated and sent for microbial identification. The causative agent was confirmed as *Cercospora nicotianea*. Similarly, the *in vitro* inhibitory observables of *C. operculatus* extracts (at different concentrations) against the mycelial growth of *C. nicotianea* are shown in Figure 1 and summarized in Figure 2. Overall, all the test experiments exhibited inhibitory effects to varying degrees, while the control validated the experimental settings with no fungal inhibition. Notably, concentration C7 (9.54 mg.mL^{-1}) showed the highest inhibition effectiveness after 7 days of fungal inoculation; otherwise, those with lower concentrations were recorded with gradual activity attenuation. On day 3 post-inoculation, all the concentrations of *C. operculatus* extract were found to exhibit potent disinfecting capacity (100% inhibition). On day 5 post-inoculation, the inhibitory potential was in the following order: C6 (88.89%) > C5 (76.19%) > C4-C1 (ca. 60%). On day 7 post-inoculation, all the test samples, except for C7 (100%), exhibited inhibition < 80%.
GC-MS analysis of *C. operculatus* extract revealed 22 components, of which 21 (**1-21**) were identifiable from the NIST-17 database. The results are summarised in Table 1, and the corresponding formulae are shown in Figure 3. From the results, 4',5'-dimethoxy-2'-hydroxy-4-methylchalcone was the most predominant compound (**21**; 41.71 %) of the extract, followed by phytol (**15**; 8.46 %), and 5.7-dimethoxyflavanone (**20**; 5.20 %). These constitute the major part of the extract. Therefore, further evaluation of their activity is of exceptional importance. Besides, 2,3-dihydro-5-hydroxy-6,8.8-trimethyl-2-phenyl-4H-1-benzopyran-4.7-(8H)-dione (**19**; 3.67 %), caryophyllene oxide (**9**; 3.04%), 2,4-dihydroxy-3,6-dimethyl benzoic

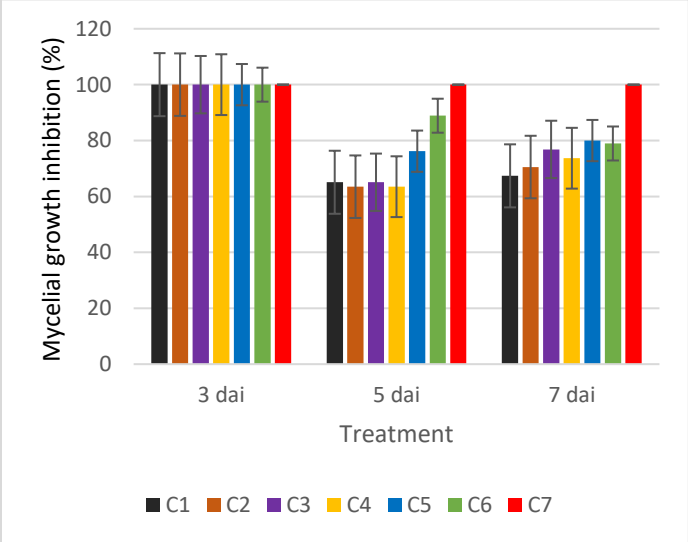

Figure 1: Antifungal effect of *C. operculatus* extracts on the mycelial growth of *C. nicotianea*; C1: 2.24, C2: 3.39, C3: 4.57, C4: 5.77, C5: 7.00; C6: 8.26; C7: 9.54 (unit: mg.mL^{-1}, $p \leq 0.05$, dai: days after inoculation)

The bio-inhibitory activities of the putative compounds as potential inhibitors (**1-21**) were assessed by their static complexes formed with a representative protein structure (Q6DQW3) through docking studies. In general, this can serve as their preliminary interaction with specific protein targets rather than a rigid conclusion. The effectiveness can be ranked according to the total docking score (DS) values (representing Gibbs free energy of a ligand-protein structure formation) and the number of hydrogen-like bonds (responsible for ligand-protein intermolecular interaction). Screening over the protein crystal (MOE algorithms), the four most susceptible sites to the ligands were determined; their parameters corresponding to each ligand-protein duo are summarised in Table 2. On average, the most inhibitory structures were in the following order: 19-Q6DQW3 ($\overline{DS}$ -10.7 kcal.mol^{-1}; DS_{max} -12.7 kcal.mol^{-1}) > 21-Q6DQW3 ($\overline{DS}$ -10.3 kcal.mol^{-1}; DS_{max} -11.9 kcal.mol^{-1}) > 20-Q6DQW3 ($\overline{DS}$ -10.3 kcal.mol^{-1}; DS_{max} -11.7 kcal.mol^{-1}); the maximum number of hydrogen-like bonds are all 3. The values are of elevated significance, cf. that of **D** ($\overline{DS}$ -10.7 kcal.mol^{-1}; DS_{max} -11.1 kcal.mol^{-1}). Mancozeb is a well-known multi-site fungicide against a broad range of fungal enzymes (especially those with sulfhydryl groups).[35] In general, these were evaluated as considerably competent compared to the results retrieved in our previous works on theoretical compounds consisting of robust antimicrobial activity against other agricultural fungi (*Rhizoctonia solani* and *Magnaporthe oryzae*), i.e., silver[36] and copper[37] tetrylenes. Coupled with the findings from the compositional analysis, also constituting *C. operculatus*-extract major

portion means that they are more likely to be primarily responsible for the antifungal properties

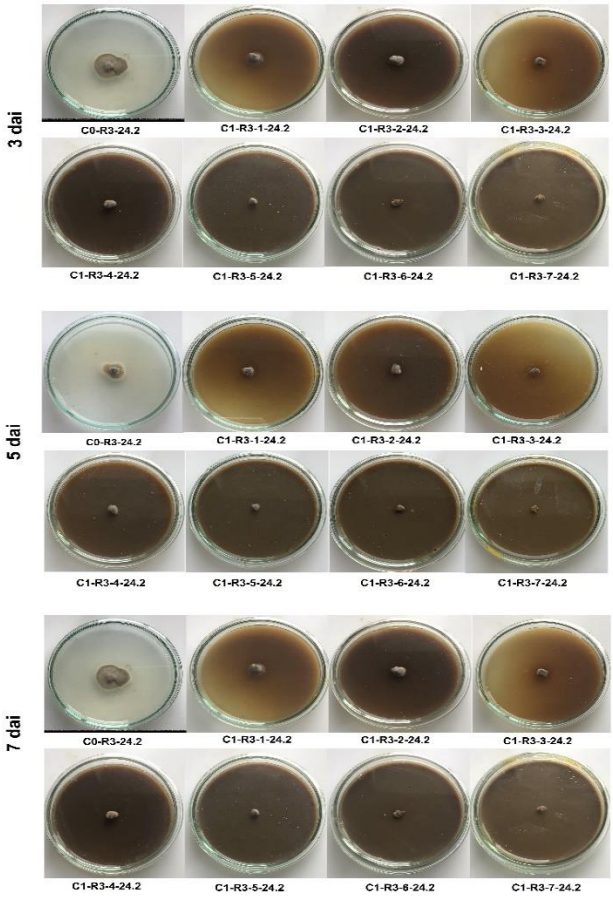

Figure 2: *In vitro* assays of *C. operculatus* extracts on the mycelial growth of *C. nicotianea* (dai: days after inoculation)

acid ethyl ester (**1**; 2.59 %), palmitic acid (**13**; 2.18%), and cetene (**8**; 2.01%) accounting for ca. 15% of the extract are also considerable to certain extent.

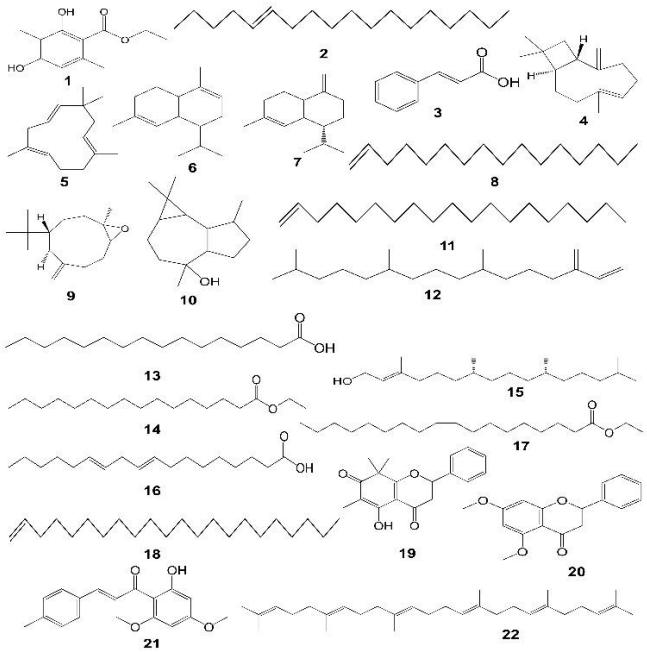

Figure 3: Chemical structures of compounds (**1-22**) in *C. operculatus* ethanol extract

observed; thus, the unknown agent is less likely to serve a pronounced role. In contrast, although **15** contributes a moderate quantitative percentage, it does not seem to contribute a corresponding biological activity. The ligand-protein inhibitory configurations for the most stable inhibitory systems are rendered for visual presentation in Figure 4. Apparently, all the ligands, in general, have good bio-conformational fitness with the in-site morphological features of the protein given by the continuous contours in the 2D interaction maps. Also, all the inhibited sites seem to be rather tight cf. the inhibitor sizes. This might advance the steric hindrance, promoting the ligand confinement yet discouraging further size-elevating functionalisation. In-detail bonding parameters corresponding to these duo complexes are summarised in Table S2. The bio-medium compatibility and intermolecular interactability of the potential inhibitors can be perceptually interpreted based on their *ab initio* insights in the scope of quantum calculation. Unlike docking-based models, these properties are regarded as the intrinsic properties of the candidates (**1-21**) without the reliance on external structures. The structures optimised for geometry are presented in Figure 5. The input structures can be readily self-consistently converged during computational iterations without encountering any geometrical constraints or unusual bonding parameters (i.e., angles and lengths). This process somewhat confirms the origin of the compounds, which are typically acknowledged to exist in a stable state in nature.

The typical ground state energy and dipole moment are summarised in Table 3. In theory, the former indicates the overall chemical reactivity of a molecular structure, while the latter offers insights into its potential for dipole-dipole interactions. On the one hand, a more stable molecule is preferred for inhibitory applications because it is expected to maintain its chemical structure and properties during the physio-medium transport before approaching the biological targets, thereby likely preserving its biological activities. Hence, the constituents in order of most favorableness are **22** (-1172.77 a.u.) > **21** ≈ **19** (approx. -1000 a.u.) > **20** (-ca. -950 a.u.). On the other hand, a greater dipole moment indicates that the host molecule would exhibit greater compatibility with a dipole-solvent environment, such as physiological or chemical media. This argumentation is followed by the order for the uppermost interest, i.e., **19** (7.14 Debye) > **21** (6.48 Debye). The results reveal that *C. operculatus*-extract major components (especially **19** and **21**) also possess supportive chemical properties for a promising bio-inhibitor.

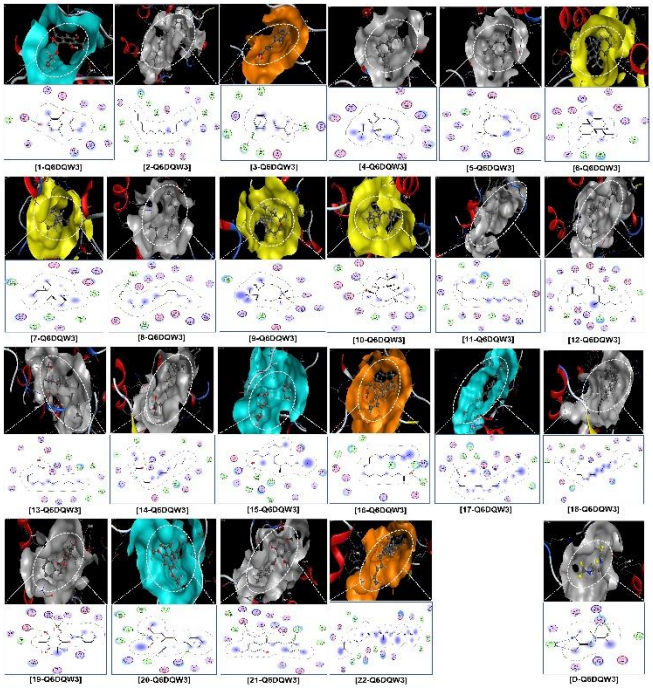

Figure 4: Visual arrangement and interaction map of L-Q6DQW3 (L: **1-22** and **D**) inhibitory structures; dashed arrow: hydrogen-like bonding, blurry purple: van der Waals interaction, dashed contour: conformational fitness

Table 1: Bioactive compounds identified in *C. operculatus* ethanol extract

Notation	Retention time (min)	Substance	Formula	Percentage (%)
1	5.73	Benzoic acid, 2,4-dihydroxy-3,6-dimethyl-,ethyl acetate	$C_{11}H_{14}O_4$	2.59
2	5.97	5-octadecene	$C_{18}H_{36}$	1.38
3	6.24	Trans-cinnamic acid	$C_9H_8O_2$	1.18
4	6.30	Caryophyllene	$C_{15}H_{24}$	1.22
5	6.54	Humelene	$C_{15}H_{24}$	0.59
6	6.62	1-isopropyl-4,7-dimethyl-1,2,4a,5,6,8a-hexahydronaphthalene	$C_{15}H_{24}$	0.51
7	6.65	δ-Muurolene	$C_{15}H_{24}$	0.50
8	7.27	Cetene	$C_{16}H_{32}$	2.01
9	7.33	Caryophyllene oxide	$C_{15}H_{24}O$	3.04
10	7.59	Globulol	$C_{15}H_{26}O$	0.92
11	8.42	1-nonadecene	$C_{19}H_{39}$	1.51
12	8.66	Neophyltadiene	$C_{20}H_{38}$	1.47
13	9.30	Palmitic acid	$C_{16}H_{32}O_2$	2.18
14	9.47	Palmitic acid, ethyl ester	$C_{18}H_{36}O_2$	1.05
15	10.06	Phytol	$C_{20}H_{40}O$	8.46
16	10.18	9,12-octadecadienoic acid	$C_{18}H_{32}O_2$	0.93
17	10.31	Ethyl oleate	$C_{20}H_{38}O_2$	0.48
18	10.42	1-docosene	$C_{22}H_{44}$	0.49
19	11.39	2,3-dihydro-5-hydroxy-6,8,8-trimethyl-2-phenyl-4H-1-benzopyran-4,7(8H)-dione	$C_{18}H_{18}O_4$	3.67
20	12.16	Flavanone, 5,7-dimethoxy-	$C_{17}H_{16}O_4$	5.20
-	12.41	Unknown	-	17.23
21	12.76	4',6'-dimethoxy-2'-hydroxy-4-methylchalcone	$C_{18}H_{18}O_4$	41.71
22	13.11	Squalene	$C_{30}H_{50}$	1.66

Table 2. Screening results on inhibitability of complexes **L-Q6DQW3** (L: **1-22** and **D**)

L	Site 1		Site 2		Site 3		Site 4		
	E	**N**	**E**	**N**	**E**	**N**	**E**	**N**	$\overline{\mathbf{DS}}$
1	-9.3	1	-11.0	2	-7.1	0	-8.4	1	-9.0
2	-6.5	0	-7.0	0	-7.1	0	-7.8	0	-7.1
3	-7.8	1	-9.5	2	-12.7	4	-9.0	2	-9.8
4	-6.7	0	-6.9	0	-7.0	0	-7.2	0	-7.0
5	-6.0	0	-7.0	0	-7.8	0	-7.1	0	-7.0
6	-7.2	0	-7.2	0	-6.3	0	-7.4	0	-7.0
7	-7.3	0	-6.0	0	-6.3	0	-6.8	0	-6.6
8	-6.1	0	-7.1	0	7.2	0	-8.6	1	-3.7
9	-9.9	2	-8.2	1	-8.0	1	-7.6	0	-8.4
10	-10.3	2	-6.9	0	-7.1	0	-6.5	1	-7.7
11	-6.7	0	-7.3	0	-6.9	0	-7.7	0	-7.2
12	-7.0	0	-7.2	0	-7.9	0	-8.2	0	-7.6
13	-6.2	1	-7.0	1	-7.3	1	-11.6	2	-8.0
14	-7.0	0	-8.0	1	-6.7	0	-8.3	1	-7.5
15	-7.3	1	-10.5	2	-8.0	1	-7.9	0	-8.4
16	-7.7	1	-6.1	0	-10.4	2	-7.0	0	-7.8
17	-6.2	0	-9.6	1	-7.0	0	-7.6	0	-7.6
18	-6.8	0	-7.0	0	-6.7	0	-7.1	1	-6.9
19	-11.2	2	-9.9	1	-8.8	1	-12.7	3	-10.7
20	-8.9	1	-11.7	3	-9.0	1	-10.9	2	-10.1
21	-9.8	1	-10.0	1	-8.9	1	-11.9	3	-10.2
22	-6.7	0	-6.0	0	-7.2	0	-7.0	0	-6.7
D	-10.8	4	-9.2	2	-10.2	3	-11.1	6	-10.3

DS: DS value (kcal.mol^{-1}); $\overline{\mathbf{DS}}$: Average DS values of different sites (kcal.mol^{-1}); **N**: Number of hydrophilic interactions

The molecular electrostatic potential (MEP) distributions are shown in Figure 6. Essentially, these configurations are based on the electronic density distributed at various regions of the molecular plane. This visualisation can be a basis for assessing molecular flexibility when interacting with external structures, particularly those with irregular or

arbitrary surface features. The analysis results showed that all molecules appear to localise their electron distribution around their electrophilic groups (i.e., oxygen-based functionality). Noticeably, the negative-positive difference of **21** is most significant at ca. $\pm 8\times10^{-2}$ a.u., marking the highest capacity to create hydrogen-like bonds via its oxygen atoms. Similar justifications can be applied for **19** and **20**, other major components, with marginally lower dipole moment values (ca. $\pm 6\times10^{-2}$ a.u.).

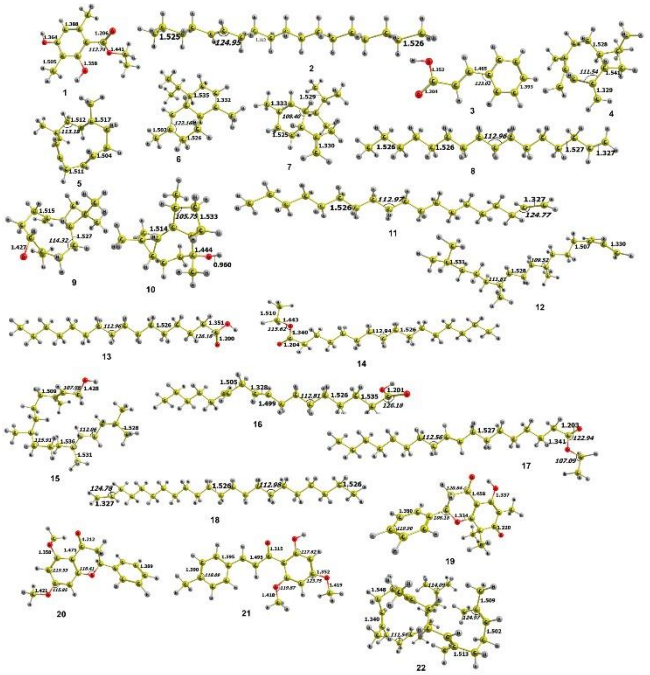

Figure 5: Geometrically optimised structures of **1-22**; length (Å), angle (°)

Table 3: Ground state electronic energy and dipole moment values of **1-22**

Compound	Ground state electronic energy (a.u.)	Dipole moment (Debye)
1	-728.63	2.46
2	-707.67	0.02
3	-498.30	3.26
4	-584.83	0.79
5	-546.74	0.73
6	-586.11	0.39
7	-586.10	0.69
8	-629.03	0.50
9	-661.30	2.47
10	-662.55	1.84
11	-746.99	0.48
12	-785.08	0.51
13	-779.57	1.57
14	-858.19	2.33
15	-861.55	2.25
16	-855.74	2.16
17	-935.59	2.34
18	-864.94	0.50
19	-997.82	7.14
20	-958.47	2.53
21	-997.76	6.48
22	-1172.77	0.39

The physical parameters are given in Table 4. In particular, molecular mass (amu), polarizability (Å^3), size (Å), and dispersion coefficients (logP and logS) were retrieved from the QSARIS system, while the maximum number of hydrogen bonds were referenced from docking results. Overall, all compounds were considered to appropriately meet the criteria for drug-like properties according to Lipinski's guidelines; particularly, **22** (55.7 Å^3) showed the best parameters with respect to polarizability[38] (the sensitivity to polarised induction); **3** (logP 1.94) showed the most conducive value with regard to octanol-water partition [39] (the compatibility to aqueous environments). Those of *C. operculatus*-extract major components **19** (polarizability 32.0 Å^3; logP 2.30), **20** (polarizability 30.9 Å^3; logP 3.01), and **21** (polarizability 34.6 Å^3; logP 4.40) were also considered suitable for bio-medium applications. In another respect, all *C. operculatus*-extract constituents possess negative-inclined logS values, especially **18** (logS -7.53) and **21** (logS -7.55), showing they are sparingly dissolved in water. As a result, the compounds are less likely to leach out after being absorbed by the plant leaves, thus more likely prolonging the protective effects. In other words, they are expected to be more suitable with direct applications (e.g., sprayed over crops) than indirect ways (e.g., water- or soil-borne fertilisation). In general, compounds are predicted to exhibit promising physio-compatible and bio-persistent pesticides.

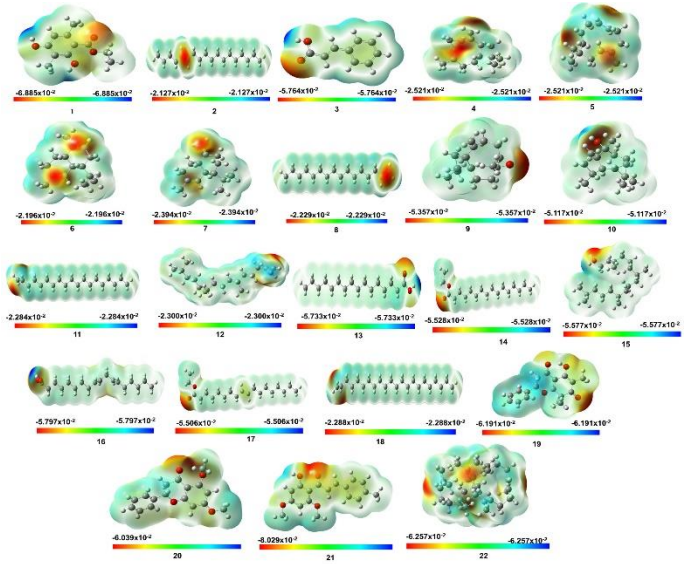

Figure 6: Molecular electrostatic potential (MEP) map of **1-22**; reddish region: negative electrostatic potential, bluish region: positive electrostatic potential, greenish region: null electrostatic potential

Conclusion

The study reports the component-activity correlation between *C. operculatus*-extract composition and its antifungal properties, especially against *C. nicotianae*. The pathogenic test proved the infection of *C. nicotianae* leading to the leaf-spot disease in Pennywort. The antifungal assays revealed that *C. operculatus* extract spray (9.54 mg.mL-1) can retain the full inhibition effects (100 %) against the fungi for up to 7 days after inoculation. GC-MS revealed 21 constituents, with **21, 15** and **20** as the major components. Docking simulation predicts the inhibitory effectiveness of the extract's major components, **19, 21**,

and **20**, with docking scores of -10.7 kcal.mol^{-1}; DS_{max} -12.7 kcal.mol^{-1}), -10.3 kcal.mol^{-1}; DS_{max} -11.9 kcal.mol^{-1}, and -10.3 kcal.mol^{-1}; DS_{max} -11.7 kcal.mol^{-1}, respectively. Quantum calculation also shows that the components (**22, 21**, 1**9**, **20**) possess physical compatibility, while physicochemical properties evaluation confirms the suitability of the compounds as promising physio-compatible and bio-persistent pesticides. The results indicate that *C. operculatus* extract is a promising source of inhibitory agent against *C. nicotianea*-induced leaf-spot disease in Pennywort. There is a need for further evaluation of *C. operculatus* to identify and isolate potential biopesticide agents.

Table 4: Physicochemical properties of studied compounds **1-22**

Compound	Mass	Polarizability	Size	Dispersion coefficients		Hydrogen-bond count
	(amu)	(Å^3)	(Å)	logP	logS	(Q6DQW3)
1	210.23	27.8	490.6	3.13	-3.12	2
2	252.49	33.9	530.13	4.72	-6.10	0
3	148.16	17.3	207.54	1.94	-1.89	3
4	204.36	26.4	379.38	4.01	-4.15	0
5	204.36	27.1	414.08	4.23	-4.18	0
6	204.36	26.4	387.02	4.25	-4.04	0
7	204.36	26.4	380.71	4.21	-4.03	0
8	224.40	30.1	477.67	4.68	-5.50	1
9	220.36	26.4	371.41	4.57	-4.14	2
10	222.37	26.6	53.63	4.32	-4.18	2
11	266.60	35.6	560.77	4.18	-6.44	0
12	278.50	37.2	580.77	4.63	-6.40	0
13	256.40	30.8	477.00	4.57	-4.32	2
14	284.50	34.6	546.41	4.27	-5.02	1
15	296.54	38.1	582.27	4.81	-5.13	2
16	280.40	34.5	510.54	4.24	-4.63	2
17	310.50	38.3	590.74	4.20	-5.45	1
18	308.59	41.1	47.98	5.01	-7.53	1
19	298.30	32.0	388.18	2.30	-3.32	3
20	284.30	30.9	391.83	3.01	-3.81	3
21	298.30	34.6	419.23	4.40	-7.55	3
22	310.70	55.7	803.92	4.01	-7.10	0

Conflicts of Interest

The authors declare no conflict of interest.

Authors' Declaration

The authors hereby declare that the work presented in this article are original and that any liability for claims relating to the content of this article will be borne by them.

Acknowledgments

This research was funded by the Vietnam Governmental Budget under the regulation of Thua Thien Hue province [Project No. TTH.2021-KC.12].

References

1. Gamage A, Gangahagedara R, Gamage J, Jayasinghe N, Kodikara N, Suraweera P, Merah O. Role of organic farming for achieving sustainability in agriculture. Farming Syst. 2023; 1(1):ID 100005.
2. Mfarrej MFB, Rara FM. Competitive, sustainable natural pesticides. Acta Ecol Sin. 2019;39(2):145–151.
3. Parveen S, Wani AH, Ganie AA, Pala SA, Mir RA. Antifungal activity of some plant extracts on some pathogenic fungi. Arch Phytopathol Plant Prot. 2014;47(3):279–284.
4. Botanic Gardens Conservation International (BGCI) ISGTSG. *Syzygium nervosum*. The IUCN Red List of Threatened Species. 2018.
5. Dung NX, Luu H Van, Khoi TT, Leclercq PA. GC and GC/MS analysis of the leaf oil of *Cleistocalyx operculatus* Roxb. Merr. et Perry (Syn. *Eugenia operculata* Roxb.; *Syzygium nervosum* DC.). J Essent Oil Res. 1994;6(6):661–662.
6. Prasanth MI, Sivamaruthi BS, Sukprasansap M, Chuchawankul S, Tencomnao T, Chaiyasut C. Functional properties and bioactivities of *Cleistocalyx nervosum* var. paniala berry plant: a review. Food Sci Technol. 2020;40:369–373.
7. Thuy BTP, Hieu LT, My TTA, Hai NTT, Loan HTP, Thuy NTT, Triet NT, Van Anh TT, Dieu NTX, Quy PT. Screening for *Streptococcus pyogenes* antibacterial and *Candida albicans* antifungal bioactivities of organic compounds in natural essential oils of Piper betle L., *Cleistocalyx*

operculatus L. and *Ageratum conyzoides* L. Chem Pap. 2021;75(4):1507–1519.
8. Pham TL, Doan VD, Le Dang Q, Nguyen TA, Nguyen TLH, Tran TDT, Nguyen TPL, Vo TKA, Nguyen TH. Stable biogenic silver nanoparticles from *Syzygium nervosum* bud extract for enhanced catalytic, antibacterial and antifungal properties. RSC Adv. 2023;13(30):20994–1007.
9. Gunsolus JL, Curran WS. Herbicide mode of action and injury symptoms. order. 1991;612:625–817.
10. Fodor J, Kámán-Tóth E, Dankó T, Schwarczinger I, Bozsó Z, Pogány M. Description of the *Nicotiana benthamiana* - *Cercospora nicotianae* pathosystem. Phytopathology. 2018;108(1):149–155.
11. Thomas E, Herrero S, Eng H, Gomaa N, Gillikin J, Noar R, Beseli A, Daub ME. Engineering Cercospora disease resistance via expression of *Cercospora nicotianae* cercosporin-resistance genes and silencing of cercosporin production in tobacco. PLoS One. 2020;15(3):ID e0230362.
12. Sautua FJ, Searight J, Doyle VP, Scandiani MM, Carmona MA. *Cercospora nicotianae* is a causal agent of Cercospora leaf blight of soybean. Eur J plant Pathol. 2020;156:1227–1231.
13. Zhao Q, Chen X, Liu DY, Xia CJ, Yang JG, Lv HK, Qian YM, Wang J. First report of *Cercospora nicotianae* causing frog eye spot in Cigar Tobacco in Hainan, China. Plant Dis. 2020;104(12):ID 3257.
14. Daub ME, Hangarter RP. Light-induced production of singlet oxygen and superoxide by the fungal toxin, cercosporin. Plant Physiol. 1983;73(3):855–857.
15. Beseli A, Noar R, Daub ME. Characterisation of *Cercospora nicotianae* hypothetical proteins in cercosporin resistance. PLoS One. 2015;10(10):ID e0140676.
16. Chen H, Lee M, Daub ME, Chung K. Molecular analysis of the cercosporin biosynthetic gene cluster in *Cercospora nicotianae*. Mol Microbiol. 2007;64(3):755–770.
17. Newman AG, Townsend CA. Molecular characterisation of the cercosporin biosynthetic pathway in the fungal plant pathogen *Cercospora nicotianae*. J Am Chem Soc. 2016;138(12):4219–4228.
18. Newman AG, Vagstad AL, Belecki K, Scheerer JR, Townsend CA. Analysis of the cercosporin polyketide synthase CTB1 reveals a new fungal thioesterase function. Chem Commun. 2012;48(96):11772–11774.
19. Thao TTP, Bui TQ, Quy PT, Bao NC, Van Loc T, Van Chien T, Chi NL, Van Tuan N, Van Sung T, Nhung NTA. Isolation, semi-synthesis, docking-based prediction, and bioassay-based activity of *Dolichandrone spathacea* iridoids: new catalpol derivatives as glucosidase inhibitors. RSC Adv. 2021;11(20):11959–11975.
20. Thao TTP, Bui TQ, Hai NTT, Huynh LK, Quy PT, Bao NC, Dung NT, Chi NL, Van Loc T, Smirnova IE. Newly synthesised oxime and lactone derivatives from *Dipterocarpus alatus* dipterocarpol as anti-diabetic inhibitors: experimental bioassay-based evidence and theoretical computation-based prediction. RSC Adv. 2021; 11(57):35765–35782.
21. Nguyen NPD, Quy PT, To DC, Bui TQ, Phu N V., My TTA, Nguyen PH, Kien NH, Hai NTT, Nhung NTA. Combinatory in silico study on anti-diabetic potential of *Ganoderma lucidum* compounds against α-glucosidase. Trop J Nat Prod Res. 2023;7(7):3421–3432.
22. Quy PT, Bui TQ, Bon N V, Phung PTK, Duc DPN, Nhan DT, Phu N V, To DC, Nhung NTA. *Euonymus laxiflorus* Champ. bioactive compounds inhibited α-glucosidase and protein phosphatase 1B - a computational approach towards the discovery of antidiabetic drugs. Trop J Nat Prod Res. 2023;7(5):2974–2991.
23. Sánchez-Pérez JDL, Jaimes-Lara MG, Salgado-Garciglia R, López-Meza JE. Root extracts from Mexican avocado (*Persea americana* var. drymifolia) inhibit the mycelial growth of the oomycete *Phytophthora cinnamomi*. Eur J Plant Pathol. 2009;124:595–601.
24. Pandey DK, Tripathi NN, Tripathi RD, Dixit SN. Fungitoxic and phytotoxic properties of the essential oil of *Hyptis suaveolens*. J Plant Dis Prot. 1982;89(6):344–349.
25. Molecular Operating Environment (MOE), 2022.02 Chemical Computing Group ULC, 910-1010 Sherbrooke St. W., Montreal, QC H3A 2R7, Canada, 2024.
26. Gaussian 09, Revision A.02, M. J. Frisch, G. W. Trucks, H. B. Schlegel, G. E. Scuseria, M. A. Robb, J. R. Cheeseman, G. Scalmani, V. Barone, G. A. Petersson, H. Nakatsuji, X. Li, M. Caricato, A. Marenich, J. Bloino, B. G. Janesko, R. Gomperts, B. Mennucci, H. P. Hratchian, A. F. Izmaylov, J. L. Sonnenberg, D. Williams-Young, F. Ding, J. M. Gaussian, M. Gonzalez, J. A. Pople, Gaussian, Inc., Wallingford CT, 2009.
27. Zhao Y, Schultz NE, Truhlar DG. Design of density functionals by combining the method of constraint satisfaction with parametrisation for thermochemistry, thermochemical kinetics, and noncovalent interactions. J Chem Theory Comput. 2006;2(2):364–382.
28. Reed AE, Weinstock RB, Weinhold F. Natural population analysis. J Chem Phys. 1985;83(2):735–746.
29. Cameron DR. Computer software reviews. J Am Chem Soc. 2001;123(35):8644–8645.
30. Gasteiger J, Marsili M. Iterative partial equalisation of orbital electronegativity-a rapid access to atomic charges. Tetrahedron. 1980; 36(22):3219–3228.
31. Lipinski CA, Lombardo F, Dominy BW, Feeney PJ. Experimental and computational approaches to estimate solubility and permeability in drug discovery and development settings. Adv Drug Deliv Rev. 1997;23:3–25.
32. Ahsan MJ, Samy JG, Khalilullah H, Nomani MS, Saraswat P, Gaur R, Singh A. Molecular properties prediction and synthesis of novel 1,3,4-oxadiazole analogues as potent antimicrobial and antitubercular agents. Bioorganic Med Chem Lett. 2011;21(24):7246–7250.
33. Mazumdera J, Chakraborty R, Sena S, Vadrab S, Dec B, Ravi TK. Synthesis and biological evaluation of some novel quinoxalinyl triazole derivatives. Der Pharma Chem. 2009;1(2):188–198.
34. Byrd AL, Segre JA. Adapting Koch's postulates. Science. 2016;351(6270):224–226.
35. Dall'Agnol JC, Pezzini MF, Uribe NS, Joveleviths D. Systemic effects of the pesticide mancozeb - A literature review. Eur Rev Med Pharmacol Sci. 2021;25(11):4113–4120.
36. Thuy BTP, My TTA, Hai NTT, Loan HTP, Hieu LT, Hoa TT, Bui TQ, Tuong HN, Thuy NTT, Dung DK, Van Tat P, Quy PT, Nhung NTA. A molecular docking simulation study on potent inhibitors against *Rhizoctonia solani* and *Magnaporthe oryzae* in rice: silver-tetrylene and bis-silver-tetrylene complexes vs. validamycin and tricyclazole pesticides. Struct Chem. 2021;32(1):135–148.
37. Thi Thanh Hai N, Bui TQ, Thi Ai My T, Thi Phuong Loan H, Thai Hoa T, Tu Quy P, Thi Thu Thuy N, Thanh Nhan D, Thi Ai Nhung N. In silico inhibitability of copper carbenes and silylenes against *Rhizoctonia solani* and *Magnaporthe oryzae*. J Chem. 2021;2021:ID 5555521.
38. Feynman R. The Feynman lectures on physics - Volume II. Millenium. Gottlieb MA, editor. New York: Basic Books; 2010. 11.3.
39. Sangster JM. Octanol-water partition coefficients: fundamentals and physical chemistry. Vol. 1. New Jersey: John Wiley & Sons; 1997.